

Age of Information in a SWIPT and URLLC enabled Wireless Communications System

Chathuranga M. Wijerathna Basnayaka^{†*}, Dushantha Nalin K. Jayakody[‡]
 Tharindu D. Ponnimbaduge Perera[†], Timo T Hämäläinen[§] and Mário Marques da Silva[‡]

*COPELABS, Lusófona University, Lisbon, PORTUGAL

[†]Centre for Telecommunications Research, School of Engineering, Sri Lanka Technological Campus, Padukka, SRI LANKA

[‡]Centro de Investigação em Tecnologias - Autónoma TechLab, Universidade Autónoma de Lisboa, PORTUGAL

[§] Faculty of Information Technology, University of Jyväskylä, Jyväskylä, FINLAND

Email: {chathurangab, tharindupe}@sltc.ac.lk, {djayakody, mmsilva}@autonoma.pt and timo.t.hamalainen@jyu.fi

arXiv:2211.11568v1 [cs.IT] 18 Nov 2022

Abstract—This paper estimates the freshness of the information in a wireless relay communication system that employs simultaneous wireless information and power transfer (SWIPT) operating under ultra-reliable low-latency communication (URLLC) constraints. The Age of Information (AoI) metric calculates the time difference between the current time and the timestamp of the most recent update received by the receiver is used here to estimate the freshness of information. The short packet communication scheme is used to fulfil the reliability and latency requirements of the proposed wireless network and its performance is analysed using finite block length theory. In addition, by utilising novel approximation approaches, expressions for the average AoI (AAoI) of the proposed system are derived. Finally, numerical analysis is used to evaluate and validate derived results.

Index Terms—Age of information, short-packet communication, ultra-reliable low-latency communication, simultaneous wireless information and power transfer (SWIPT).

I. INTRODUCTION

The use cases of 5G communications are classified into three broad categories: enhanced Mobile BroadBand, URLLC and mMTC. URLLC is necessary for mission-critical applications such as unmanned aerial vehicle (UAV) communication and process automation [1]–[3]. The packet size should be extremely small in URLLC to facilitate low-latency transmission. The Shannon-Hartley Capacity theorem is no longer relevant in this scenario since the law of large numbers is invalid. However, using finite block length information theory, we can derive the achievable data rate under short packet communication as a function of the SNR, the block length and the decoding error probability [4]. In addition, for these mission-critical applications, the freshness of the information is of high importance, along with the URLLC requirements. This has prompted growing interest in the age of information (AoI), a performance metric that quantifies the freshness of the information.

On the other hand, SWIPT is an emerging technology for future wireless communication systems. In general, practical SWIPT receivers for energy harvesting (EH) and information decoding have been established through the use of power splitting (PS) and time switching (TS) techniques. Since EH shares the resources allocated to information transmission, this has

an influence on the performance of wireless communication. However, minimal research has been conducted to analyse SWIPT-enabled relays using finite block length information theory and AoI.

This paper presents a wireless relay system with SWIPT for future mission-critical URLLC-enabled applications. To the best of the authors’ knowledge, no prior study has analysed AoI in a SWIPT and URLLC enabled wireless relay network. In this work, a two-way wireless relay system employs a nonlinear PS model for energy harvesting and short packet communication is employed to address the trade-off between reliability and latency. We derived an approximation for the average AoI (AAoI) of the proposed relay scheme under the finite blocklength constraint. In comparison to prior work on SWIPT, we examine the AoI performance of the proposed SWIPT system using threshold-based nonlinear EH. Furthermore, we examine the effect of various factors, including block length and packet size, on the weighed sum AAoI.

II. SYSTEM MODEL

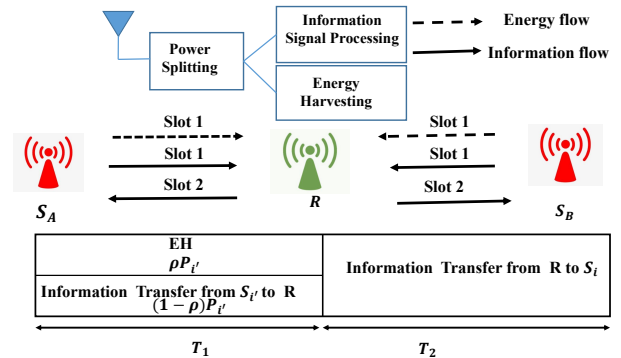


Fig. 1. In the considered system model, sources A (S_A) and B (S_B) exchange status updates with each other with the help of a single relay (R); sources send updates to the R during the first transmission time slot T_1 while the R is harvesting energy and then the R exchanges updates received from each source using harvested energy during the second transmission time slot T_2 .

This paper considers a two-way cooperative status update system where two source nodes, source A (S_A) and source

B (S_B) exchange status updates with each other as timely as possible with the help of a single relay (R). R adopts the decode-and-forward relaying protocol. Specifically, $S_i, i \in (A, B)$ transmits status updates which can be generated at the beginning of any time slot. The sources in this system are regarded as energy providers and the relay is equipped with an energy harvesting device and is capable of conducting data forwarding and harvesting energy simultaneously. In this paper, we assume R adopts the dynamic power splitting technique [5]. As shown in Fig. 1, we consider a two-time slot transmission scheme in which S_i sends updates to the R while harvesting energy during the first transmission time slot and then the R exchange updates received from S_i using harvested energy during the second transmission time slot. Specifically, $S_i, i \in (A, B)$ transmits status updates which can be generated at the beginning of any time circle following generate-at-will updates generation model [6]. Under this policy, the relay uses energy harvested within the first transmission time slot (T_1) for the transmission in the second transmission time slot (T_2) without waiting. Suppose the harvested energy is less than the minimum required energy for the transmission. In that case, the relay does not transmit received updates and updates received from both sources are destroyed at the relay. H_{ij} represents the channel coefficient of the channel between node i to node j where $i, j \in \{A, B, R\}$ and $i \neq j$. The small scale channel gain is $g_{ij} = |h_{ij}|^2$, where $h_{ij} \sim \mathcal{CN}(0, 1)$ is the Rayleigh fading channel coefficient. The probability density function (PDF) of the small scale channel gain is defined as $f_{g_{ij}}(z) = e^{-z}, z \geq 0$. The large scale channel gain α_{ij} is given by $-10 \log_{10}(\alpha_{ij}) = 20 \log_{10}(d_{ij}) + 20 \log_{10}(\frac{4\pi f_c}{c})$, where f_c, d_{ij} are the carrier frequency and distance between node i and node j respectively. c is the speed of light in the space. Thus, channel coefficient is written as $H_{ij} = \sqrt{\alpha_{ij} g_{ij}}$ and channel gain is written as $G_{ij} = \alpha_{ij} g_{ij}$. Up-link transmission between the source and the relay are performed in an orthogonal channel.

III. BLOCK ERROR ANALYSIS UNDER FINITE BLOCK-LENGTH

Our first objective is to study block error probability at each destination (opposite source) in this system. The block error probability at the destination has been derived using different mathematical approximation techniques in this section.

To calculate block error probability at each node, it is necessary to derive the SNR at each node. The received SNR at the relay from each source node $S_{i'}, i' \in \{A, B\}$ is given by,

$$\gamma_R^{i'} = \frac{(1 - \rho)P_{i'}G_{i'R}}{\sigma_R^2}, \quad (1)$$

where ρ is the power spitting factor, noise power at the relay is denoted as σ_R^2 and transmit power at the $S_{i'}$ given by $P_{i'}$. Then, the energy harvested by the relay from the each node is given by $E_R^{i'} = \rho\eta P_{i'}G_{i'R}T_1$, where η is the energy conversion efficiency and T_1 is the transmission time of the first transmission slot and it can be calculated as $T_1 = n_R^{i'}T_s$,

where $n_R^{i'}$ is the allocated block length for the transmission between i' and R and T_s is the symbol duration. Then, the total energy harvested by the relay within the first transmission slot is given by

$$E_R = \sum_{i' \in \{A, B\}} E_R^{i'} = \rho\eta T_1 (P_A G_{AR} + P_B G_{BR}). \quad (2)$$

The available energy harvested by the relay for transmission is given by

$$E_R^T = \begin{cases} E_{max} & E_R \geq E_{max} \\ E_R & E_{max} > E_R > E_{min} \\ 0 & \text{otherwise,} \end{cases} \quad (3)$$

where E_{max} is the maximum energy limit that the relay can harvest and E_{min} is the minimum energy required for transmission. E_{min} can be calculated as $E_{min} = P_{min}T_2$, where P_{min} is the minimum required power for the transmission while T_2 is the time of the second transmission slot and T_2 is calculated as $T_2 = \sum_{i \in \{A, B\}} n_i^R T_s$, where n_i^R is the allocated block length for the transmission between R and i . Then, the transmit power of relay is calculated as $P_R = \frac{E_R^T}{T_2}$. During the second time slot, the received SNR at each $S_i \in \{A, B\}$ is given by $\gamma_i = \frac{P_R G_{Ri}}{\sigma_i^2}$. Then, using (2) and (3) SNR at the destination is expressed as

$$\gamma_i = \begin{cases} \frac{E_{max} \alpha_{Ri} g_{Ri}}{T_2 \sigma_i^2}, & E_R > E_{max} \\ \frac{E_R \alpha_{Ri} g_{Ri}}{T_2 \sigma_i^2}, & E_{max} \geq E_R \geq E_{min} \\ 0, & \text{otherwise.} \end{cases} \quad (4)$$

An outage happens when the relay or opposite source are unable to decode the received message successfully. Hence, the system overall transmission success probability φ_i at each source node i can be calculated as

$$\varphi_i = 1 - \left(\varepsilon_R^{i'} + \left(1 - \varepsilon_R^{i'}\right) \varepsilon_i^R \right), \quad (5)$$

where $i \neq i', i, i' \in \{A, B\}$ and ε_j^t is the decoding error probability at receiving node $j \in (i, R)$ for block received from node $t \in (i', R)$. Due to the static nature of the communication channels, it is assumed that the fading coefficients stay constant over the duration of each transmission block. Following Polyanskiy's results on short packet communication [4] and assuming that the receiver has the perfect channel state information, the expectation of the block error probability at the receiving node for a given block length n_j^t can be written as

$$\varepsilon_j^t = \mathbb{E} \left[Q \left(\frac{n_j^t C(\gamma_j^t) - k_j^t}{\sqrt{n_j^t V(\gamma_j^t)}} \right) \right], \quad (6)$$

where $\mathbb{E}[\cdot]$ is the expectation operator, $Q(x) = \frac{1}{\sqrt{2\pi}} \int_x^\infty e^{-\frac{t^2}{2}} dt$ and $V(\gamma_j^t)$ is the channel dispersion, which can be written $V(\gamma_j^t) = \frac{\log_2^2 e}{2} \left(1 - \frac{1}{(1 + \gamma_j^t)^2}\right)$. The variable $C(\gamma_j^t)$ denotes the channel capacity of a complex AWGN channel and it is given by $C(\gamma_j^t) = \log_2(1 + \gamma_j^t)$. The

number of bits per block represents by k_j^t . Moreover, under the Rayleigh fading channel conditions, ε_j^t can be formulated as

$$\varepsilon_j^t = \int_0^\infty f_{\gamma_j^t}(z) Q\left(\frac{n_j^t C(\gamma_j^t) - k_j^t}{\sqrt{n_j^t V(\gamma_j^t)}}\right) dz, \quad (7)$$

where $f_{\gamma_j^t}(z)$ denotes the PDF of the received SNR (γ_j^t) at the receiving node j . Due to the complexity of the Q-function, it is challenging to get a closed-form expression for the overall decoding error probability. Thus, using the approximation technique given in [7] and [8], (7) can be approximated as $\varepsilon_j^t \approx \int_0^\infty f_{\gamma_j^t}(z) \Theta_j^t(z) dz$, where $\Theta_j^t(z)$ denotes the linear approximation of $Q\left(\frac{n_j^t C(\gamma_j^t) - k_j^t}{\sqrt{n_j^t V(\gamma_j^t)}}\right)$, this can be expressed as in [8]

$$\Theta_j^t(z) = \begin{cases} 1, & \gamma_j^t \leq \phi_j^t, \\ \frac{1}{2} - \beta_j^t \sqrt{n_j^t} (\gamma_j^t - \psi_j^t), & \phi_j^t < \gamma_j^t < \delta_j^t, \\ 0, & \gamma_j^t \geq \delta_j^t, \end{cases} \quad (8)$$

where $\beta_j^t = \frac{1}{2\pi \sqrt{2^{\frac{2k_j^t}{n_j^t}} - 1}}$, $\psi_j^t = 2^{\frac{k_j^t}{n_j^t}} - 1$, $\phi_j^t = \psi_j^t - \frac{1}{2\beta_j^t \sqrt{n_j^t}}$ and $\delta_j^t = \psi_j^t + \frac{1}{2\beta_j^t \sqrt{n_j^t}}$. By using above linear approximation ε_j^t can be expressed as

$$\varepsilon_j^t \approx \beta_j^t \sqrt{n_j^t} \int_{\phi_j^t}^{\delta_j^t} F_{\gamma_j^t}(z) dz, \quad (9)$$

where $F_{\gamma_j^t}(z)$ denotes the CDF of the received SNR (γ_j^t) at receiving node j . To calculate success probability at each source i using (5), it is necessary to calculate ε_i^R and ε_i^t . Using (8) and (9) block error probabilities at the R and each source can be calculated as follows,

$$\varepsilon_i^t \approx \beta_i^t \sqrt{n_i^t} \int_{\phi_i^t}^{\delta_i^t} F_{\gamma_i^t}(z) dz, \quad (10)$$

$$\varepsilon_i^R \approx \beta_i^R \sqrt{n_i^R} \int_{\phi_i^R}^{\delta_i^R} F_{\gamma_i^R}(z) dz. \quad (11)$$

Lemma 1. An approximation for the block error probability at the relay is derived as

$$\varepsilon_i^R \approx 1 - \left(\frac{(1-\rho)P_{i'}\alpha_{i'R}\beta_{i'}^R \sqrt{n_{i'}^R}}{\sigma_R^2} \right) \left(e^{-\frac{\phi_{i'}^R \sigma_R^2}{(1-\rho)P_{i'}\alpha_{i'R}}} - e^{-\frac{\delta_{i'}^R \sigma_R^2}{(1-\rho)P_{i'}\alpha_{i'R}}} \right). \quad (12)$$

Proof. The PDF of SNR at relay from each source can be calculated using (1) as $f_{\gamma_{i'}^R}(x) = \frac{\sigma_R^2}{(1-\rho)P_{i'}\alpha_{i'R}} e^{-\frac{x\sigma_R^2}{(1-\rho)P_{i'}\alpha_{i'R}}}$. Then, the CDF can be calculated as

$$F_{\gamma_{i'}^R}(z) = 1 - e^{-\frac{z\sigma_R^2}{(1-\rho)P_{i'}\alpha_{i'R}}}. \quad (13)$$

Then, the result can be proved by substituting (13) to (10). \square

Lemma 2. Block error probability at the opposite receiving node can be derived as follows:

$$\varepsilon_i^R \approx \beta_i^R \sqrt{n_i^R} \left(\left(\frac{\delta_i^R + \phi_i^R}{2} \right) \sum_{v=1}^V \frac{\pi}{V} \sqrt{1 - \phi_v^2} F_{\gamma_i^R}(q) + R_V \right) \quad (14)$$

where $\phi_v = \cos\left(\frac{2v-1}{2v}\pi\right)$, $q = \left(\frac{\delta_i^R - \phi_i^R}{2}\right)\phi_v + \left(\frac{\delta_i^R + \phi_i^R}{2}\right)$, V is the complexity-accuracy trade-off factor, while R_V denotes the error term, which is ignored at substantially larger values of V .

Proof. To calculate error probability at S_i , it is necessary to derived the CDF of SNR. Using (3), $F_{\gamma_i^R}(z)$ is evaluated as

$$\begin{aligned} F_{\gamma_i^R}(z) &= \mathbb{P}_r(\gamma_i^R < z) = 1 - \mathbb{P}_r\{E_R \geq E_{min} \cap \gamma_i^R > z\} \\ F_{\gamma_i^R}(z) &= 1 - \underbrace{\mathbb{P}_r\{E_{min} \leq E_R \leq E_{max} \cap \gamma_i^R > z\}}_{L_1} \\ &\quad - \underbrace{\mathbb{P}_r\{E_R \geq E_{max} \cap \gamma_i^R > z\}}_{L_2}. \end{aligned} \quad (15)$$

Then, substituting $E_R = \rho\eta T_1(P_A\alpha_{ARGAR} + P_B\alpha_{BRGBR})$ into (15), L_1 is evaluated as

$$L_1 = \mathbb{P}_r\{\Omega_1 < I < \Omega_2 \cap I g_{Ri} > \Omega_3\}, \quad (16)$$

or

$$L_1 = \begin{cases} 0, & g_{Ri} < \frac{\Omega_3}{\Omega_2}, \\ \mathbb{P}_r\left\{\frac{\Omega_3}{g_{Ri}} < I \leq \Omega_2\right\}, & \frac{\Omega_3}{\Omega_2} < g_{Ri} < \frac{\Omega_3}{\Omega_1}, \\ \mathbb{P}_r\{\Omega_1 < I \leq \Omega_2\}, & g_{Ri} > \frac{\Omega_3}{\Omega_1}, \end{cases} \quad (17)$$

where $\Omega_1 = \frac{E_{min}}{\rho\eta T_1}$, $\Omega_2 = \frac{E_{max}}{\rho\eta T_1}$, $\Omega_3 = \frac{z\sigma_R^2 T_2}{\rho\eta T_1 \alpha_{Ri}}$ and $I = \sum_{i \in \{A,B\}} P_i \alpha_{iR} g_{iR}$. To calculate L_1 it is necessary to get PDF and CDF of I and g_{Ri} . Then, to calculate the PDF of I , it is considered as summation of two independent random variable as $I = \mu_1 + \mu_2$, where $\mu_1 \sim \exp\left(\frac{1}{P_A\alpha_{AR}}\right)$ and $\mu_2 \sim \exp\left(\frac{1}{P_B\alpha_{BR}}\right)$. Using the concepts of convolution of random variables, PDF and CDF of I can be calculated as follows:

$$\begin{aligned} f_I(z) &= \int_{-\infty}^{\infty} f_{\mu_1}(x) f_{\mu_2}(z-x) dx, \\ &= \int_0^z \frac{1}{P_A\alpha_{AR}} e^{-\frac{1}{P_A\alpha_{AR}}x} \frac{1}{P_B\alpha_{BR}} e^{-\frac{1}{P_B\alpha_{BR}}(z-x)} dx, \\ &= \frac{1}{P_A\alpha_{AR} P_B\alpha_{BR}} e^{-\frac{1}{P_B\alpha_{BR}}z} \int_0^z e^{(\frac{1}{P_B\alpha_{BR}} - \frac{1}{P_A\alpha_{AR}})x} dx, \\ f_I(z) &= \begin{cases} \frac{1}{P_A\alpha_{AR} - P_B\alpha_{BR}} (e^{-\frac{1}{P_A\alpha_{AR}}z} - e^{-\frac{1}{P_B\alpha_{BR}}z}), \\ \text{if } \frac{1}{P_A\alpha_{AR}} \neq \frac{1}{P_B\alpha_{BR}}, \\ \frac{1}{(P_A)z} z e^{-\frac{1}{P_A}z}, & \text{if } \frac{1}{P_A\alpha_{AR}} = \frac{1}{P_B\alpha_{BR}} = \frac{1}{P_A}, \end{cases} \quad (18) \end{aligned}$$

where f denotes the PDF function of a random variable. Then, the CDF of I can be calculated as

$$F_I(z) = P(Z \leq z) = \int_0^z f(t)dt,$$

$$F_I(z) = \begin{cases} 1 + \frac{P_B \alpha_{BR}}{P_A \alpha_{AR} - P_B \alpha_{BR}} e^{-\frac{z}{P_B \alpha_{BR}}} \\ - \frac{P_A \alpha_{AR}}{P_A \alpha_{AR} - P_B \alpha_{BR}} e^{-\frac{z}{P_A \alpha_{AR}}}, \\ \text{if } P_A \alpha_{AR} \neq P_B \alpha_{BR}, \\ 1 - e^{-\frac{1}{P_A} z} \left(1 + \frac{1}{P_A} z\right) \text{ if } \frac{1}{P_A \alpha_{AR}} = \frac{1}{P_B \alpha_{BR}} = \frac{1}{P_A}, \end{cases} \quad (19)$$

Further, we derive the approximation for L_1 as follows,

$$L_1 = \int_{\frac{\Omega_3}{\Omega_2}}^{\frac{\Omega_3}{\Omega_1}} \left(f_{g_{Ri}}(x) \int_x^{\Omega_2} f_I(y) dy \right) dx \\ + \int_{\Omega_1}^{\Omega_2} f_I(x) dx \int_{\frac{\Omega_3}{\Omega_1}}^{\infty} f_{g_{Ri}}(x) dx, \quad (20)$$

$$L_1 = L_3 + (F_I(\Omega_2) - F_I(\Omega_1)) \left(1 - F_{Ri}\left(\frac{\Omega_3}{\Omega_1}\right)\right),$$

where

$$L_3 = \int_{\frac{\Omega_3}{\Omega_2}}^{\frac{\Omega_3}{\Omega_1}} \left(f_{g_{Ri}}(x) \int_x^{\Omega_2} f_I(y) dy \right) dx, \\ = \int_{\frac{\Omega_3}{\Omega_2}}^{\frac{\Omega_3}{\Omega_1}} f_{g_{Ri}}(x) \left[F_I(\Omega_2) - F_I\left(\frac{\Omega_3}{x}\right) \right] dx, \quad (21) \\ L_3 = F_I(\Omega_2) \left[F_{g_{Ri}}\left(\frac{\Omega_3}{\Omega_1}\right) - F_{g_{Ri}}\left(\frac{\Omega_3}{\Omega_2}\right) \right] - L_4,$$

where L_4 is defined as

$$L_4 = \int_{\frac{\Omega_3}{\Omega_2}}^{\frac{\Omega_3}{\Omega_1}} f_{g_{Ri}}(x) F_I\left(\frac{\Omega_3}{x}\right) dx, \quad (22)$$

Using Gaussian-Chebyshev-Quadrature (GCQ) method [9], (22) can be approximated as follows,

$$L_4 \approx \frac{\frac{\Omega_3}{\Omega_1} + \frac{\Omega_3}{\Omega_2}}{2} \sum_{m=1}^M \frac{\pi}{M} \sqrt{1 - \phi_m^2} f_{g_{Ri}}(z_1) F_I\left(\frac{\Omega_3}{z_1}\right) + R_M, \quad (23)$$

where $\phi_m = \cos\left(\frac{2m-1}{2M}\pi\right)$, $z_1 = \frac{\frac{\Omega_3}{\Omega_1} - \frac{\Omega_3}{\Omega_2}}{2} \phi_m + \frac{\frac{\Omega_3}{\Omega_1} + \frac{\Omega_3}{\Omega_2}}{2}$, M is the complexity-accuracy trade-off factor, and R_M is the error term that can be ignored at sufficiently high M values. Finally, expression for L_1 can be approximated as shown in (24). Similarly, L_2 is calculated as

$$L_2 = \mathbb{P}_r \{I > \Omega_2 \cap g_{Ri} > \Omega_4\} \\ = (1 - F_I(\Omega_2)) (1 - F_{g_{Ri}}(\Omega_4)), \quad (26)$$

where $\Omega_4 = \frac{z \sigma_i^2 T_2}{E_{max} \alpha_{Ri}}$. Then, CDF of SNR at each destination ($F_{g_{Ri}}(z)$) can be obtained by substituting (24) and (26) in (15) as in (25). Then, the result can be proved by substituting (25) to (9) and then applying the GCQ method for the integration of the CDF function. \square

Finally, substituting (12) and (14) into (5) the overall transmission success probability can be calculated.

IV. AGE OF INFORMATION ANALYSIS

This section estimates the AAOI of the two-way relay system. This system adopts the generate-at-will update generation model [6]. Hence, S_A and S_B generate new status updates every transmission cycle to keep the information at the corresponding destinations as fresh as possible. Then, generated updates are transmitted to their opposite sources using a relay system. If the generation time of the freshest update received at opposite source time stamp t is $g(t)$, then AoI can be defined as a random process as $\Delta(t) = t - g(t)$. As illustrated in the Fig.2, it is assumed that at $t = 0$ the measurements of the AoI starts and the AoI at the opposite source (destination) is set to $\Delta(0) = \Delta_0$. Each source generates updates at time stamps g_1, g_2, \dots, g_{n-1} and the opposite source receive these updates at time stamps g_2, g_3, \dots, g_n . As illustrated in Fig.2, data update i is transmitted from the source at time stamp $t = g_i$ and it is successfully delivered to its opposite source at time stamp $g_{i+1} = g_i + T$ where T is total time allocated for a one transmission circle and $T = T_1 + T_2$. Therefore, if update packet delivered successfully, at the time g_{i+1} , the AoI at the opposite source is estimated as $\Delta(g_{i+1}) = T$. We assume that AoI increases linearly until the next update is successfully delivered to the opposite source. As an example, one packet fails to be decoded at time g_3 , hence, $\Delta(t)$ continues to increase linearly. For the considered time period T_c , time average AoI can be computed using the area under $\Delta(t)$. Similarly, the time average age is estimated as $\Delta_{T_c} = \frac{1}{T_c} \int_0^{T_c} \Delta(t) dt$. Similar to the work presented in [10], the time average age (Δ_{T_c}) tends to ensemble average age when $T_c \rightarrow \infty$, i.e., which can be expressed as

$$\Delta^{AAOI} = \mathbb{E}[\Delta] = \lim_{t \rightarrow \infty} \mathbb{E}[\Delta(t)] = \lim_{T_c \rightarrow \infty} \Delta_{T_c}. \quad (27)$$

Applying graphical methods to saw-tooth age waveform in Fig.2 and using [1, eq.8] we can calculate AAOI at each $S_i, i \in (A, B)$ as follows:

$$\Delta_i^{AAOI} = \frac{E[X_i^2]}{2E[X_i]} + T, \quad (28)$$

where X_i denote the inter departure time between two consecutive successfully received status updates at S_i . It assumes that the end-to-end delay of each successfully received update is always a constant, which is given by $E[Y_i] = T_1 + T_2 = T$. The inter departure time X_i is a geometric random variable with mean $E[X_i] = \frac{T}{\varphi_i}$ and second moment $E[X_i^2] = \frac{T^2(2-\varphi_i)}{\varphi_i^2}$.

Lemma 3. For the two way relay network, the expression of the AAOI at each source can be obtained as follows:

$$\Delta_i^{AAOI} = \frac{T}{2} + \frac{T}{\varphi_i}. \quad (29)$$

Proof. The result can be proved by substituting $E[X_i] = \frac{T}{\varphi_i}$ and $E[X_i^2] = \frac{T^2(2-\varphi_i)}{\varphi_i^2}$ into (28). \square

The expected weighted sum AAOI of the two-way relay system can be calculated as follows, $\Delta_{Sum}^{AAOI} = \sum_{i \in \{A, B\}} \omega_i \Delta_i^{AAOI}$, where ω_i is the weighting coefficient at S_i .

$$L_1 \approx F_I(\Omega_2) \left[F_{g_{Ri}} \left(\frac{\Omega_3}{\Omega_1} \right) - F_{g_{Ri}} \left(\frac{\Omega_3}{\Omega_2} \right) \right] - \frac{\Omega_3 + \frac{\Omega_3}{\Omega_2}}{2} \sum_{m=1}^M \sqrt{1 - \phi_m^2} f_{g_{Ri}}(z_1) F_I \left(\frac{\Omega_3}{z_1} \right) + R_M + (F_I(\Omega_2) - F_I(\Omega_1)) \left(1 - F_{g_{Ri}} \left(\frac{\Omega_3}{\Omega_1} \right) \right). \quad (24)$$

$$F_{\gamma_i^R}(z) \approx 1 - F_I(\Omega_2) \left[F_{g_{Ri}} \left(\frac{\Omega_3}{\Omega_1} \right) - F_{g_{Ri}} \left(\frac{\Omega_3}{\Omega_2} \right) \right] - \frac{\Omega_3 + \frac{\Omega_3}{\Omega_2}}{2} \sum_{m=1}^M \sqrt{1 - \phi_m^2} f_{g_{Ri}}(z_1) F_I \left(\frac{\Omega_3}{z_1} \right) + R_M + (F_I(\Omega_2) - F_I(\Omega_1)) \left(1 - F_{g_{Ri}} \left(\frac{\Omega_3}{\Omega_1} \right) \right) - (1 - F_I(\Omega_2)) (1 - F_{g_{Ri}}(\Omega_4)). \quad (25)$$

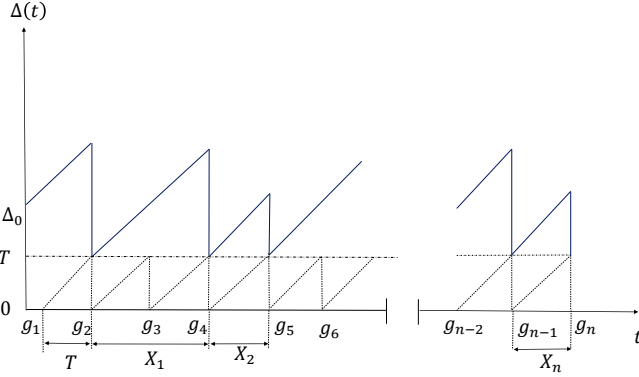


Fig. 2. Evolution of AoI $\Delta(t)$ with the time: Each source generate updates at time stamps g_1, g_2, \dots, g_{n-1} and the opposite source receive these updates at time stamps g_2, g_3, \dots, g_n ; $\Delta(t)$ is the AoI at the opposite source (destination).

V. SIMULATION RESULTS AND DISCUSSIONS

In this section, we present the analytical and numerical simulation results. Unless otherwise stated, the simulation parameters are set as: $d_{AR} = 30$ m, $d_{BR} = 30$ m, $f_c = 900$ MHz, speed of the light (m/s) $= 3 \times 10^8$ ms⁻¹, $P_A = 1$ W, $P_B = 1$ W, $T_s = 20$ μ s, $n_R^A, n_R^B = 200$ bits, $n_A^R, n_B^R = 200$ bits, $k_R^A, k_R^B = 32$ bits, noise power $(\sigma_R^2, \sigma_A^2, \sigma_B^2) = -100$ dBm, $E_{max} = 0.001$ J, $P_{min} = 0.0001$ mW, $\rho = 0.5$, $\omega_A = 0.5$, $\omega_B = 0.5$ and energy $\eta = 0.9$.

The weighted sum of AAoI as a function of transmission power in Fig. 3 for different distances is derived. The weighted sum of AAoI decreases dramatically as the transmit power at the sources increases, since increasing the transmit power at the source reduces the error probability at the relay node and increases the amount of energy harvested by the relay. However, for large transmission power levels, the AAoI value is fixed since the number of erroneous packets that impact the AAoI is too small. On the other hand, when the distance between the relay and sources is short, the AAoI is low, and when the distance increases, the AAoI increases due to low SNR. The numerically simulated AAoI well coincides with the approximated results, especially moderate SNR values, since the linear approximation applied in (8) is too tight for moderate

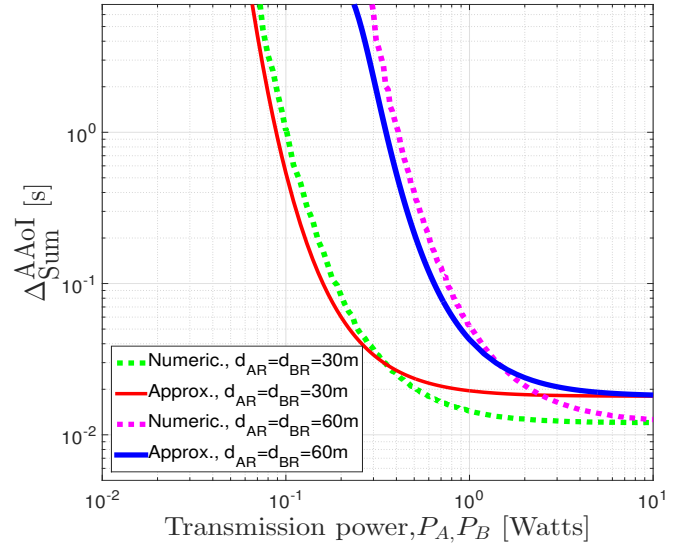


Fig. 3. Weighed sum AAoI as a function of transmission power

SNR values [11]. Next, in Fig. 4, we plot the weighted sum AAoI versus block length. When the transmission power is high, AAoI increases when block length is increased, as the number of erroneous packets is too low under high SNR conditions and increasing block length only increases transmission time. However, under low-SNR scenarios, small block length increases AAoI due to the high block error probability and increasing block length towards its optimal value decreases the AAoI due to the decrease in error probability. On the other hand, increasing the block length after the optimal value has resulted in an increase in AAoI because the impact of transmission time on AAoI is greater than the decrease in block error probability. This result proved that a short block length does not always maintain information freshness. In Fig. 5 we present the weighed sum AAoI versus update size. If the transmission power is low, the AAoI increases as the packet size increases under fixed block length since it increases the overall block error probability. However, in high SNR scenarios, packet size has little effect on AAoI since block

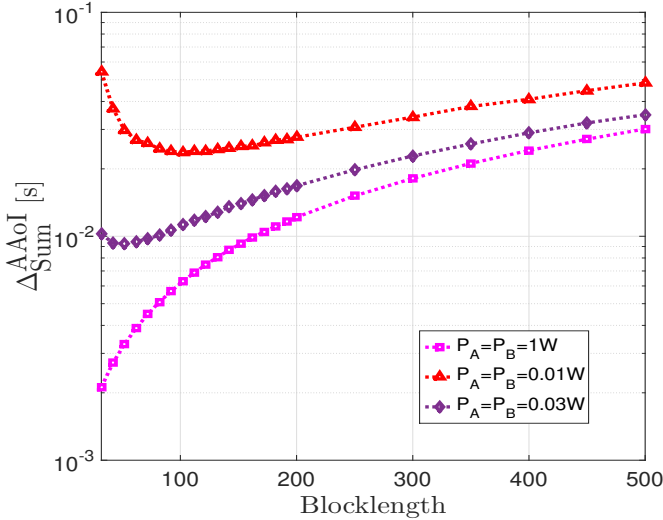


Fig. 4. Weighed sum AAoI as a function of block length.

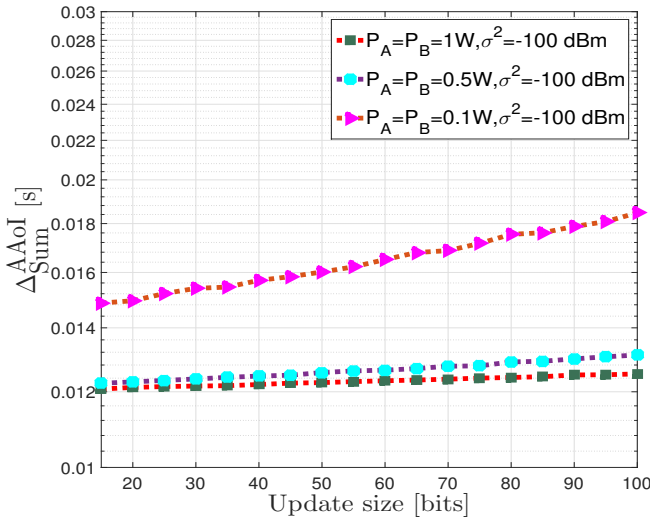


Fig. 5. Weighed sum AAoI as a function of update size.

error probability is low. Fig. 6 illustrates the weighted sum AAoI as a function of P_{min} . The weighted sum AAoI of the system is monotonically increasing with the P_{min} since high P_{min} threshold values increase update loss at the relay.

VI. CONCLUSIONS

This work developed a model to estimate the AAoI in a two-way relay equipped with SWIPT that operates under ultra-reliable and low latency constraints. We derived an approximation for AAoI at each source using linear approximation techniques. The impacts of various parameters was studied, i.e., including block length, packet size, transmission power and noise level. Then, the numerical analysis to evaluate and validate the derived results. We observed that packet size does not affect freshness when SNR is high. Short packet communication retains an improved AoI performance in low

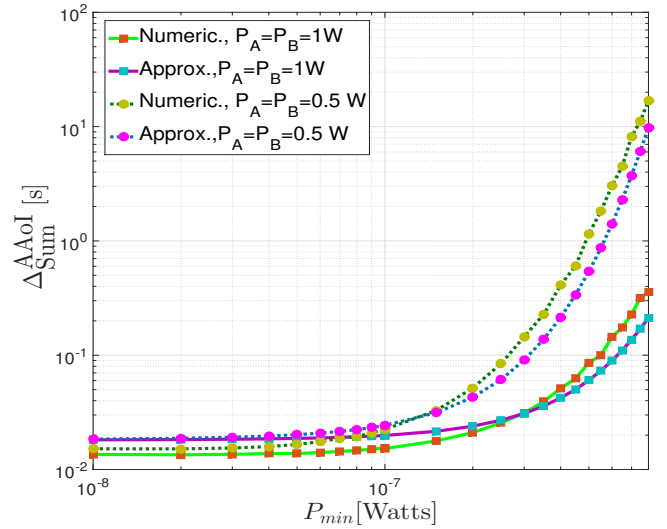


Fig. 6. Weighed sum AAoI as a function of P_{min} .

SNR scenarios. This paper concludes that the short block length communications does not always assist in maintaining freshness in SWIPT-enabled communications systems, even though it always assists in maintaining a low latency.

VII. ACKNOWLEDGEMENT

This work is funded by the CEU-Cooperativa de Ensino Universitário, Portugal.

REFERENCES

- [1] C. M. W. Basnayaka, D. N. K. Jayakody, and Z. Chang, "Age of information based URLLC-enabled UAV wireless communications system," *IEEE Internet Things J.*, 2021.
- [2] A. Sharma, P. Vanjani, N. Paliwal, C. M. W. Basnayaka, D. N. K. Jayakody, H.-C. Wang, and P. Muthuchidambaramanathan, "Communication and networking technologies for UAVs: A survey," *J. Netw. Comput. Appl.*, p. 102739, 2020.
- [3] T. D. P. Perera, D. N. K. Jayakody, I. Pitas, and S. Garg, "Age of information in swipt-enabled wireless communication system for 5g," *IEEE Wirel. Commun.*, vol. 27, no. 5, pp. 162–167, 2020.
- [4] Y. Polyanskiy, H. V. Poor, and S. Verdú, "Channel coding rate in the finite blocklength regime," *IEEE Trans. Inf. Theory*, vol. 56, no. 5, pp. 2307–2359, 2010.
- [5] T. D. P. Perera, D. N. K. Jayakody, S. K. Sharma, S. Chatzinotas, and J. Li, "Simultaneous wireless information and power transfer (SWIPT): Recent advances and future challenges," *IEEE Commun. Surv. Tutor.*, vol. 20, no. 1, pp. 264–302, 2017.
- [6] E. T. Ceran, D. Gündüz, and A. Gyöngy, "Average age of information with hybrid ARQ under a resource constraint," *IEEE Trans. Wirel. Commun.*, vol. 18, no. 3, pp. 1900–1913, 2019.
- [7] B. Makki, T. Svensson, and M. Zorzi, "Finite block-length analysis of the incremental redundancy HARQ," *IEEE Wireless Commun. Lett.*, vol. 3, no. 5, pp. 529–532, 2014.
- [8] Y. Gu, H. Chen, Y. Li, and B. Vucetic, "Ultra-reliable short-packet communications: Half-duplex or full-duplex relaying?" *IEEE Wireless Commun. Lett.*, vol. 7, no. 3, pp. 348–351, 2017.
- [9] M. Abramowitz, I. A. Stegun, and R. H. Romer, "Handbook of mathematical functions with formulas, graphs, and mathematical tables," 1988.
- [10] A. Kosta, N. Pappas, and V. Angelakis, "Age of information: A new concept, metric, and tool," *Found. Trends Netw.*, vol. 12, no. 3, pp. 162–259, 2017.
- [11] C. M. W. Basnayaka, D. N. K. Jayakody, T. D. P. Perera, and M. V. Ribeiro, "Age of information in an URLLC-enabled decode-and-forward wireless communication system," in *2021 IEEE 93rd Veh. Technol. Conf. (VTC2021-Spring)*. IEEE, 2021, pp. 1–6.